(*Washington, D.C.*) *228*, 291-297.
Crawford, I. P., Decastel, M., & Goldberg, M. E. (1978) *Biochem. Biophys. Res. Commun. 85*, 309-316.
Crawford, I. P., Nichols, B. P., & Yanofsky, C. (1980) *J. Mol. Biol. 142*, 489-502.
Fairwell, T., & Breuer, H. B. (1979) *Anal. Biochem. 99*, 242-248.
Fairwell, T., & Breuer, H. B. (1980) *Anal. Biochem. 107*, 140-149.
Hathaway, G. M., & Crawford, I. P. (1970) *Biochemistry 9*, 1801-1808.
Hayashi, R. (1977) *Methods Enzymol. 47*, 84-93.
Higgins, W., Fairwell, T., & Miles, E. W. (1979) *Biochemistry 18*, 4827-4834.
Higgins, W., Miles, E. W., & Fairwell, T. (1980) *J. Biol. Chem. 255*, 512-517.
Högberg-Raibaud, A., & Goldberg, M. E. (1977a) *Biochemistry 16*, 4014-4019.
Högberg-Raibaud, A., & Goldberg, M. E. (1977b) *Proc. Natl. Acad. Sci. U.S.A. 74*, 442-446.
Jekel, P. A., Weijer, W. J., & Beintema, J. J. (1983) *Anal. Biochem. 134*, 347-354.
Kubo, K., Isemura, T., & Takagi, T. (1982) *Biochim. Biophys. Acta 703*, 180-186.
Laemmli, U. K. (1970) *Nature (London) 227*, 680-685.
Lee, H.-M., & Riordan, J. F. (1978) *Biochem. Biophys. Res. Commun. 85*, 1135-1142.
Little, J. W., & Hill, S. A. (1985) *Proc. Natl. Acad. Sci. U.S.A. 82*, 2301-2305.
Martin, B., Svendsen, I., & Ottesen, M. (1977) *Carlsberg Res. Commun. 42*, 99-102.
Miles, E. W., & Higgins, W. (1978) *J. Biol. Chem. 253*, 6266-6269.
Miles, E. W., Yutani, K., & Ogasahara, K. (1982) *Biochemistry 21*, 2586-2592.
Miles, E. W., Bauerle, R., & Ahmed, S. A. (1986) *Methods Enzymol.* (in press).
Neurath, H. (1980) in *Protein Folding* (Jaenicke, Ed.) pp 501-523, Elsevier/North-Holland Biomedical Press, Amsterdam, New York.
Richardson, J. S. (1981) *Adv. Protein Chem. 34*, 167-339.
Rocha, V., Brennan, E. F., & Plumb, S. (1979) *Arch. Biochem. Biophys. 193*, 34-41.
Schenkein, I., Levy, M., Franklin, E. C., & Frangione, B. (1977) *Arch. Biochem. Biophys. 182*, 64-70.
Shirahama, K., Tsujii, K., & Takagi, T. (1974) *J. Biochem. (Tokyo) 75*, 309-319.
Steffens, G. J., Giinzler, W. A., Otting, F., Frankus, E., & Flohe, L. (1982) *Hoppe-Seyler's Z. Physiol. Chem. 363*, 1043-1058.
Takagi, T., Tsujii, K., & Shirahama, K. (1975) *J. Biochem. (Tokyo) 77*, 939-947.
Tschopp, J., & Kirschner, K. (1980) *Biochemistry 19*, 4521-4527.
Tsunasawa, S., Yutani, K., Ogasahara, K., Taketani, M., Yasuoka, N., Kakudo, M., & Sugino, Y. (1983) *Agric. Biol. Chem. 47*, 1391-1395.
Tung, J.-S., & Knight, C. A. (1971) *Biochem. Biophys. Res. Commun. 42*, 1117-1121.
Watson, J. D. (1976) in *Molecular Biology of the Gene*, 3rd ed., pp 327-329, Benjamin, Menlo Park, CA.
Wetlaufer, D. B. (1981) *Adv. Protein Chem. 34*, 61-92.

Soluble Fibrin–Fibrinogen Complexes as Intermediates in Fibrin Gel Formation

Jacob Wilf[‡] and Allen P. Minton*

Section on Pharmacology, Laboratory of Biochemical Pharmacology, National Institute of Arthritis, Diabetes, and Digestive and Kidney Diseases, National Institutes of Health, Bethesda, Maryland 20892

Received July 8, 1985; Revised Manuscript Received January 30, 1986

ABSTRACT: Oligomer formation in fibrinogen solutions following addition of thrombin was studied by addition of thrombin inhibitor at various times subsequent to thrombin, followed by size-exclusion chromatography (SEC) on a high-performance SEC column capable of resolving species of molecular weights $\leq 10^6$. Peaks corresponding to species with 1, 2, 3, and 4 or more times the molecular weight of fibrinogen were detected and quantified via nonlinear least-squares curve-fitting procedures. The evolution of each of these peaks with time is well accounted for by a kinetic model in which the predominant component of each oligomeric molecular weight species is a linear complex of fibrinogen and fibrin. The observed predominance of trimeric over dimeric oligomers even at short times suggests that the thrombin-catalyzed release of the two A fibrinopeptides from a single molecule of fibrinogen is highly cooperative.

Numerous studies of the thrombin-catalyzed conversion of fibrinogen to fibrin and the concomitant formation of fibrin gels have been carried out with the intention of elucidating the mechanism of fibrin gel formation [for a recent review, see Scheraga (1983)]. Time-dependent studies carried out under quasi-physiological conditions, as monitored by a variety of techniques (Ferry & Morrison, 1947; Shinowara, 1966; Brass et al., 1976; J. Wilf and A. P. Minton, unpublished results) have shown two distinctly different types of kinetics, depending upon the concentration of thrombin which is added to initiate the reaction. In the presence of high concentrations of thrombin, the characteristic time for appearance of a gel following addition of thrombin decreases monotonically with increasing fibrinogen concentration. In contrast, at low concentrations of thrombin, the characteristic time goes through a minimum at some intermediate value of fibrinogen concentration and increases significantly at higher fibrinogen concentrations. Although this biphasic behavior has been

* Address correspondence to this author at the National Institutes of Health, Building 8, Room 226, Bethesda, MD 20205.
[‡] Present address: 26 Habanai Street, Jerusalem 96264, Israel.

noted by several investigators, its mechanistic implications have been largely overlooked, with the exception of Brass et al. (1976), who suggested that the existence of an optimal fibrinogen concentration could be qualitatively accounted for by the hypothesis that fibrin oligomerization is retarded at high fibrinogen concentration by the formation of stable soluble complexes between fibrin and fibrinogen.

The existence of stable soluble noncovalently linked complexes of fibrinogen and fibrin, first proposed by Shainoff and Page (1962), has been the subject of some debate in the literature (Sasaki et al., 1966; Yudelman et al., 1974; Krell et al., 1979; Smith, 1980). By and large, chromatographic experiments undertaken to ascertain the presence (or absence) of such complexes have been performed on solutions that are considerably different both in composition and in the method of preparation from those used in the kinetic experiments, having been prepared by mixing fibrinogen with fibrin solubilized from a clot by the addition of chaotropic agents such as urea. The sole exception of which we are aware is the study of Smith (1980), who performed size-exclusion chromatography on solutions, initially containing only fibrinogen, which were subjected to the action of thrombin for various periods of time prior to the introduction of a thrombin inhibitor.

In the present work we employ high-performance size-exclusion columns, which have a resolution at least 3 times greater than columns used in previous studies, to measure the fractional abundances of small oligomers formed following the addition of thrombin to fibrinogen solutions under quasi-physiological conditions, as functions of the duration of thrombin action. In contrast to previous studies, contributions of individual molecular weight species to the experimentally obtained chromatogram are quantified by computer-aided deconvolution, and the degree of oligomerization of a particular species (through trimer) is unambiguously identified by the elution volume of the associated peak. The results are compared with the predictions of several quantitative kinetic models for oligomer formation at short times following addition of thrombin, and it is found that, among the models investigated, both the current results and those previously reported by Smith (1980) are best accounted for by a model which allows fibrinogen molecules to associate with and "cap" the ends of a linear fibrin oligomer.

Materials and Methods

Materials

Bovine fibrinogen (>98% clottable) was obtained from Behring Diagnostics. Following dissolution in distilled water, the protein was dialyzed against a buffer comprising 0.05 M sodium citrate, 0.15 M sodium chloride, and 1 mM ethylenediaminetetraacetic acid adjusted to pH 7.5 at 20 °C. Following clarification by filtration through glass fibers, fibrinogen concentration was determined spectrophotometrically by using a standard absorbance of 15.1 dL g^{-1} cm^{-1} at 280 nm. At least 96% of the total absorbance at 280 nm of fibrinogen solutions so prepared eluted in a single narrow peak from the HPLC size-exclusion column described below.

Human thrombin (3000 NIH units/mg) and leech hirudin (1000 units/mg) were obtained from Sigma. Proteins used as molecular weight markers were obtained in marker kits from Pharmacia. Whole salmon sperm DNA was a gift from Dr. A. Furano, NIH. All other chemicals were reagent grade, and water was glass distilled.

Methods

High-Performance Size-Exclusion Chromatography. Solutions were chromatographed isocratically at room temperature (25 ± 1 °C) on a 300 × 7.5 mm Toyo Soda TSK-4000SW silica-based size-exclusion column with a solvent flow rate of 0.5 mL/min unless otherwise noted. Elution of solutes was monitored spectrophotometrically. The resolving power of the column, calculated from the elution volume and peak width at half-height of an elution peak of copper sulfate, ranged between 16000 and 24000 theoretical plates per meter for several different columns used during the course of this investigation. The resolving power of any given column tended to decrease with increasing length of service, but this may have been a result of the unconventional nature of the solutions being chromatographed (as will be described).

Text experiments were carried out with the TSK 4000SW column with no precolumn, with a 10-cm TSK 2000SW precolumn, and with a 4-cm Brownlee Aquapore AP-GU precolumn. The use of a precolumn did not appear to alter the qualitative nature of the resulting chromatographic separation and increased the duration of useful service of a given TSK 4000SW column. However, the installation of a precolumn did result in a decrease in the resolution of separation; the number of theoretical plates per meter typically dropped 10–30% depending upon the individual precolumn and analytical column. Because TSK 4000SW columns are costly and relatively fragile, we preferred to use precolumns when the resolution obtained was sufficient to permit us to carry out the measurements and analysis to be described.

A calibration curve for each column was constructed via the following procedure. The elution volumes of several protein molecular weight standards were measured, along with those of a small molecule, assumed to elute in the salt volume, and two large polymers, assumed to elute in the void volume. To these data was fitted an empirical relation based upon a cylindrical pore model (Ackers, 1970):

$$v(M) = v_0 + (v_s - v_0)[1 - (M/M_{max})^{1/n}]^2 \qquad M < M_{max}$$
$$v(M) = v_0 \qquad M \le M_{max} \qquad (1)$$

where $v(M)$ is the elution volume of a solute of molecular weight M, v_0 is the void volume of the column, v_s is the salt volume, and n and M_{max} are fitting parameters. Equation 1 was found to provide a satisfactory fit to the data for all columns used, but the best-fit values of the parameters varied from column to column, particularly when precolumns were used. A sample set of calibration data points is plotted in Figure 1, along with the functional relationship calculated with eq 1 together with the best-fit parameter values given in the figure caption. Inspection of the data and the best-fit function indicates that, with some care, it is possible to experimentally resolve individual macromolecular species having molecular weights as high as 1×10^6.

Chromatography of Aggregates Formed during Early Stages of Fibrin Formation. At time zero, a small amount (<10 μL) of thrombin solution was added with mixing to 1 mL of fibrinogen solution thermostated at the desired temperature. The solution thus prepared contained 7.2 mg/mL fibrinogen and 1.0 unit/mL thrombin. At time Δt, a small amount (<10 μL) of solution containing a 6-fold excess of hirudin over the amount of previously added thrombin was added and the solution mixed again. Within a few seconds, 20 μL of the solution was injected into the HPLC apparatus, and the resulting elution profile (A_{280} as a function of elapsed time or volume) was recorded digitally to facilitate subsequent data processing.

Experimental Results and Data Analysis

Chromatography of Aggregates Formed following Addition of Thrombin to Fibrinogen. Chromatograms obtained after

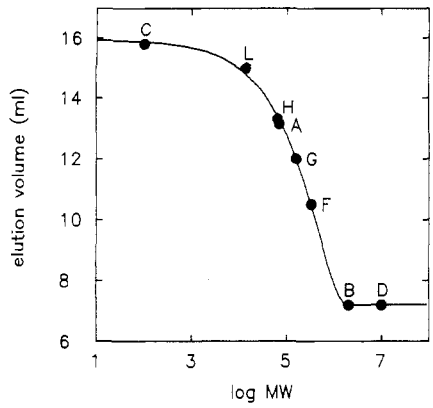

FIGURE 1: Calibration curve for a TSK 4000SW SEC column. Calibrating solutes used are the following, in order of increasing molecular weight: copper sulfate (C); lysozyme, M_r 14K (L); hemoglobin, M_r 65K (H); bovine serum albumin, M_r 70K (A); γ-globulin, M_r 160K (G); fibrinogen, M_r 330K (F); blue dextran, $M_r \sim 2\,000\,000$ (B); and salmon sperm DNA, $M_r \sim 10\,000\,000$ (D). Best-fit parameters used in eq 1 to generate the calibration curve are $v_0 = 7.20$, $v_s = 15.95$, $n = 1.82$, and $M_{max} = 1.84 \times 10^6$.

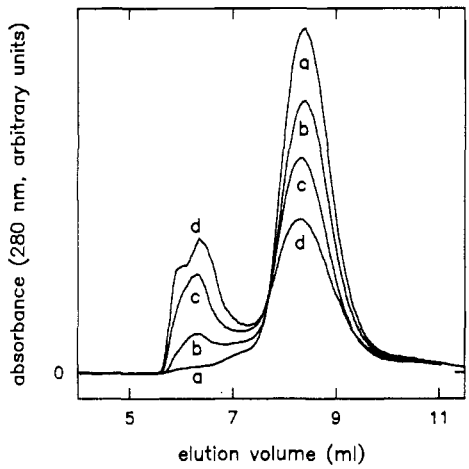

FIGURE 2: Size-exclusion chromatograms of fibrinogen/fibrin solutions (0.72 mg/mL) following action of thrombin (1.0 unit/mL) for the following times (Δt): (a) 0 s; (b) 60 s; (c) 120 s; (d) 180 s.

inhibition of thrombin at times Δt = 0, 60, 120, and 180 s are superimposed in Figure 2. For clarity, chromatograms obtained at Δt = 20, 40, 80, 100, 140, and 160 s are not shown but were analyzed together with those shown (see below). The total integrated absorbance eluting from the column was constant to within ±5% up to Δt = 180 s but at longer times began to diminish markedly, indicating that aggregates above a certain size are trapped in the column. These aggregates could only be removed by flushing the column with a dissociating agent such as 20% urea.

To quantitatively characterize a chromatogram, we employ a model function that represents the functional dependence of absorbance A upon elution volume v as a sum of peaks associated with individual eluting species i:

$$A(v) = \sum_i A_i(v) \qquad (2a)$$

The major peak associated with fibrinogen or monomeric fibrin (i = 1) is modeled by an asymmetric Gaussian function:

$$A_1(v) = h_1 \exp\left[-2.773\left(\frac{v - v_1}{w_{1a}}\right)^2\right] \quad v < v_1$$
$$A_1(v) = h_1 \exp\left[-2.773\left(\frac{v - v_1}{w_{1b}}\right)^2\right] \quad v \geq v_1 \qquad (2b)$$

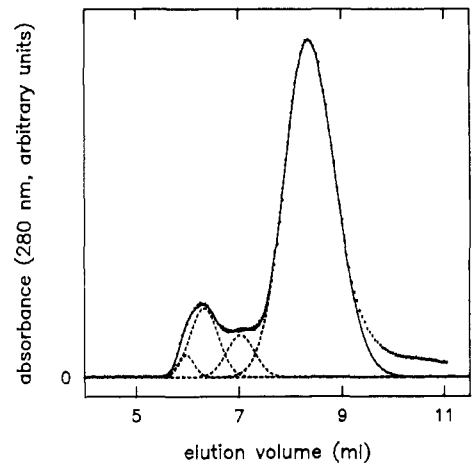

FIGURE 3: Best fit of eq 2a–c (solid curve) to chromatographic data for t = 80 s (points). The four individual Gaussian components are plotted as dashed curves.

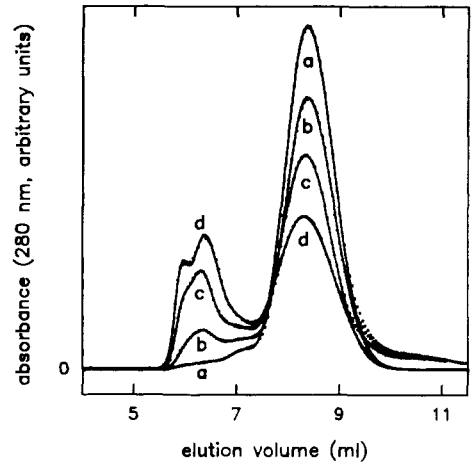

FIGURE 4: Continuous curves are simulated chromatographic patterns calculated by using eq 2a–c with parameter values given in Table I for Δt = (a) 0, (b) 60, (c) 120, and (d) 180 s. Points are the corresponding data sets shown in Figure 2.

All peaks eluting ahead of this peak are modeled by standard Gaussian functions:

$$A_i(v) = h_i \exp\left[-2.773\left(\frac{v - v_i}{w_i}\right)^2\right] \quad \text{for } i > 1 \qquad (2c)$$

In eq 2a–c, h_i represents the maximum height of peak i, v_i represents the elution volume corresponding to the maximum of peak i, and w_i (or the mean of w_{1a} and w_{1b}) is the width of peak i at half-maximum height. The asymmetric Gaussian function was selected to model peak 1 after it was found that a symmetric Gaussian could not fit the peak to within experimental uncertainty.

By use of a Marquardt–Levenberg nonlinear least-squares curve-fitting procedure (Magar, 1972), eq 2a–c were fit to each chromatographic data set individually to obtain the best-fit values of the v_i, h_i, and w_i (including w_{1a} and w_{1b}). The chromatograms for $\Delta t \leq 40$ s could be satisfactorily fitted by a model function containing three Gaussian functions (peaks), while those for $\Delta t > 40$ s required the inclusion of a fourth peak. The results of fitting a four-Gaussian function to the data for Δt = 80 s are shown in Figure 3, together with the contributions from each Gaussian to the fitted sum of Gaussians. The values of best-fit parameters and the estimated uncertainty of peak positions are presented in Table I. In Figure 4, the functions calculated by using eq 2a–c together

Table I: Best-Fit Values of Parameters Obtained by Nonlinear Least-Squares Fitting of Equations 2a–c to Size-Exclusion Chromatographic Data As Described in Text[a]

	peak 1			peak 2			peak 3			peak 4		
Δt (s)	v_1 (mL)	h_1	w_{1a}/w_{1b} (mL)	v_2 (mL)	h_2	w_2 (mL)	v_3 (mL)	h_3	w_3 (mL)	v_4 (mL)	h_4	w_4 (mL)
0	8.36	1596	0.97/1.20	7.08	65.0	0.46	6.50	36.8	0.99			
20	8.34	1516	0.89/1.24	7.16	96.9	0.58	6.42	72.1	0.87			
40	8.43	1475	0.97/1.20	7.17	114	0.59	6.41	122	0.76			
60	8.35	1261	0.96/1.24	7.07	130	0.72	6.35	165	0.60	6.01	54.3	0.36
80	8.34	1134	1.03/1.24	7.04	142	0.63	6.33	234	0.64	6.00	78.0	0.36
100	8.36	1035	1.04/1.28	7.10	168	0.74	6.36	357	0.64	5.97	102	0.30
120	8.32	996	1.05/1.23	6.98	185	0.74	6.28	442	0.60	5.93	149	0.28
140	8.28	907	1.04/1.37	7.03	190	0.73	6.34	502	0.65	5.94	237	0.33
160	8.42	870	1.12/1.43	6.95	261	0.87	6.43	456	0.62	6.06	234	0.32
180	8.30	715	1.06/1.50	7.03	163	0.59	6.37	620	0.69	5.91	310	0.28
$\langle v_i \rangle$	8.35 ± 0.05			7.06 ± 0.07			6.38 ± 0.06			5.97 ± 0.05		

[a] Also shown is mean ± 1 S.E.M. of elution volume corresponding to the maximum of each peak. Values of h_i are in arbitrary relative units.

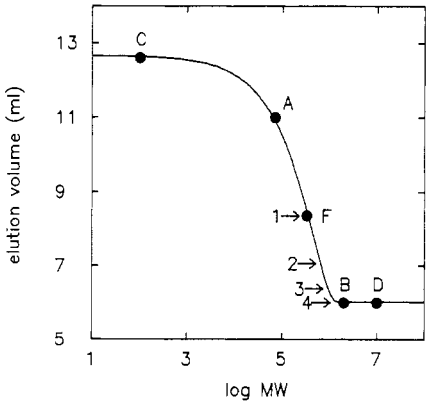

FIGURE 5: Calibration curve for a TSK 4000SW SEC column, with average best-fit elution volumes of peaks 1–4 indicated by arrows. Best-fit values of the parameters used in eq 1 to generate the calibration curve are $v_0 = 6.02$, $v_s = 12.67$, $n = 1.54$, and $M_{max} = 1.42 \times 10^6$. Molecular weights corresponding to the best-fit peak positions given in Table I, calculated from the calibration curve, are 3.5 (±0.1) × 10^5, 6.5 (±0.2) × 10^5, 9.4 (±0.4) × 10^5, and ≥1.42 × 10^6, respectively.

with the best-fit parameter values for Δt = 0, 60, 120, and 180 s are plotted together with the respective data sets. The agreement between best-fit functions and all data sets (not just those shown) is excellent, except for a tail eluting behind peak 1 which we did not attempt to model.

Examination of the results summarized in Table I reveals that the elution volume of each of these peaks is independent of Δt to within experimental error (±0.1 mL). The mean values of each of the v_i are indicated in Figure 5. Using the best-fit calibration function plotted in Figure 4, we calculate that peaks 1–4 are associated respectively with species having molecular weights approximately equal to 1, 2, 3, and 4 or more times that of fibrinogen. These species will be henceforth referred to respectively as monomer, dimer, trimer, and tetramer+.

The area under a given Gaussian component is proportional to the product of its maximum height and its width at half-maximum height. When the total area summed over all peaks was normalized to unity, the fractional abundance of material eluting in each peak was calculated for each value of Δt and is plotted as a function of Δt in Figure 6a. The results of a second independent experiment performed with a different preparation of fibrinogen (concentration 9.0 mg/mL) are plotted in Figure 6b, and the two sets of results may be seen to be in semiquantitative agreement. Of particular interest is the finding that the amount of material present as trimer increases as rapidly or more rapidly than the amount present as dimer even at small values of Δt and that the amount of

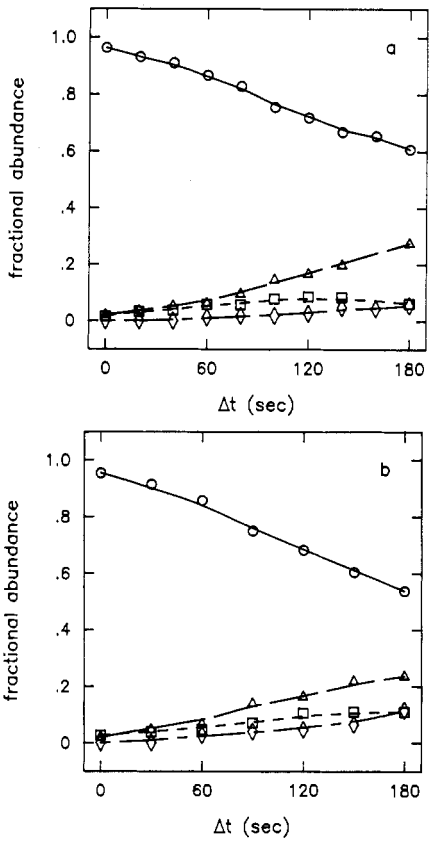

FIGURE 6: Fractional abundance of monomer (circles), dimer (squares), trimer (triangles), and tetramer+ (diamonds) as a function of Δt. Points are derived from chromatographic data as described in the text. Continuous smooth curves are drawn through each data set. Parts a and b show results obtained from two separate experiments.

dimer levels off at about 10% maximum, whereas the amount of trimer continues to increase to about 25% at Δt = 180 s.

Kinetic Model for Oligomer Formation following Addition of Thrombin. We have attempted to simulate the observed dependence of the fractional abundances of monomer, dimer, trimer, and tetramer+ upon Δt using a simple kinetic model based upon the following assumptions:

(1) The cleavage of fibrinopeptide B is neglected as a second-order effect upon oligomer formation at early times following the addition of thrombin (Shainoff & Page, 1962; Blombäck et al., 1978; Martinelli & Scheraga, 1980).

(2) Both A peptides are assumed to be removed from a fibrinogen molecule by thrombin in a highly cooperative fashion; i.e., the species containing a single A peptide is negligible. Justification for this assumption will be presented

under Discussion. The species with and without A peptides are respectively referred to as fibrinogen (denoted by G) and fibrin (denoted by F).

(3) The rate constant for association of a monomer with another monomer or with an oligomer is assumed to be independent of oligomer size.

(4) For the purpose of calculting the concentrations of species formed at short times following the addition of thrombin, associations between two oligomers are assumed to be negligible relative to associations between monomer and another monomer or oligomer. Justification for this assumption will be presented under Discussion.

(5) The dissociation of complexes formed is assumed to be negligible over the time course of the simulation.

(6) Oligomers formed in early stages of aggregation are assumed to be linear, i.e., can grow in a maximum of two directions (Blombäck et al., 1978).

(7) Fibrinogen may associate with a reactive site with a rate constant α times that for association of fibrin with a reactive site.

(8) Thrombin may cleave fibrinopeptide A from complexed fibrinogen molecules with a rate constant β times that for cleavage of fibrinopeptide A from free fibrinogen.

It follows from assumptions 6 and 7 the linear oligomers may be of three types, depicted schematically in Figure 7: F_n ($n \geq 2$), F_nG ($n \geq 1$), and GF_nG ($n \geq 1$).

Scheme I

$$G \xrightarrow{K} F \qquad F_3 + F \xrightarrow{2k} F_4$$

$$G + F \xrightarrow{2\alpha k} FG \qquad GF_2G \xrightarrow{2\beta K} F_3G$$

$$F + F \xrightarrow{2k} F_2 \qquad F_3G + G \xrightarrow{\alpha k} GF_3G$$

$$FG + G \xrightarrow{\alpha k} GFG \qquad F_3G + F \xrightarrow{k} F_4G$$

$$FG + F \xrightarrow{k} F_2G \qquad F_3G \xrightarrow{\beta K} F_4$$

$$FG \xrightarrow{\beta K} F_2 \qquad F_4 + G \xrightarrow{2\alpha k} F_4G$$

$$F_2 + G \xrightarrow{2\alpha k} F_2G \qquad F_4 + F \xrightarrow{2k} F_5$$

$$F_2 + F \xrightarrow{2k} F_3 \qquad GF_3G \xrightarrow{2\beta K} F_4G$$

$$GFG \xrightarrow{2\beta K} F_2G \qquad F_4G + G \xrightarrow{\alpha k} (GF_4G)$$

$$F_2G + G \xrightarrow{\alpha k} GF_2G \qquad F_4G + F \xrightarrow{\alpha k} (F_5G)$$

$$F_2G + F \xrightarrow{k} F_2G \qquad F_5 + G \xrightarrow{2\alpha k} (F_5G)$$

$$F_2G \xrightarrow{\beta K} F_3 \qquad F_5 + F \xrightarrow{2k} (F_6)$$

$$F_3 + G \xrightarrow{2\alpha k} F_3G$$

The above assumptions give rise to the mechanisms shown in Scheme I, which explicitly takes into account all possible oligomeric species with degree of polymerization ≤ 5. In Scheme I, K is the pseudo-first-order rate constant for conversion of uncomplexed fibrinogen to fibrin, and k is the second-order rate constant for association of a complementary site on fibrin or fibrinogen monomer with a reactive site on fibrin monomer or oligomer. A factor of 2 in a particular rate expression reflects the presence of two equivalent reactive sites (i.e., two terminal fibrin molecules in an oligomer which may react with uncomplexed monomers, or two fibrinogen protomers in an oligomer which may react with thrombin). Scheme I may be compactly portrayed as a network diagram (Figure 8).

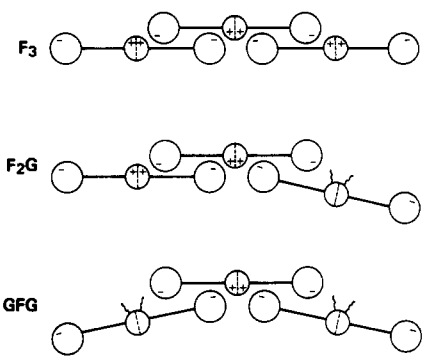

FIGURE 7: Schematic representation of the three types of oligomers postulated in the kinetic model. A fibrinogen or fibrin molecule is represented by a trinodular structure (Hall & Slayter, 1959; Fowler & Erickson, 1979). Fibrinopeptide A is represented by a threadlike projection from the central nodule, a reactive site created by cleavage of an A peptide is denoted by a (+) sign, and the complementary region of a nearest neighbor molecule in close contact with the reactive site is denoted by a (−) sign. The schematic drawings indicate that the free energy of association between a fibrinogen and a fibrin molecule is expected to be less favorable than that of association between two fibrin molecules. The extent to which differences in overall free energy of association affect the rate constant for association is manifested in the value of the parameter α.

In order to simplify the rate equations characterizing Scheme I, we define the following scaled variables: $x_A \equiv [A]/[G]^0$, where $[G]^0$ is the molar concentration of G at $t = 0$, $t' \equiv k[G]^0 t$, and $K' \equiv K/k[G]^0$.

The rate equations may then be written as functions of these variables:

$$dx_G/dt' = -x_G[K' + 2\alpha(x_F + x_{F_2} + x_{F_3} + x_{F_4} + x_{F_5}) + \alpha(x_{FG} + x_{F_2G} + x_{F_3G} + x_{F_4G})]$$

$$dx_F/dt' = K'x_G - x_F[2\alpha x_G + 2(2x_F + x_{F2} + x_{F_3} + x_{F_4} + x_{F_5}) + x_{FG} + x_{F_2G} + x_{F_3G} + x_{F_4G}]$$

$$dx_{F_2}/dt' = 2x_F^2 + \beta K'x_{FG} - 2x_{F_2}(\alpha x_G + x_F)$$

$$dx_{F_3}/dt' = 2x_F x_{F2} + \beta K'x_{F_2G} - 2x_{F_3}(\alpha x_G + x_F)$$

$$dx_{F_4}/dt' = 2x_F x_{F_3} + \beta K'x_{F_3G} - 2x_{F_4}(\alpha x_G + x_F)$$

$$dx_{F_5}/dt' = 2x_F x_{F_4} + \beta K'x_{F_4G} - 2x_{F_5}(\alpha x_G + x_F)$$

$$dx_{FG}/dt' = 2\alpha x_F x_G - x_{FG}(\alpha x_G + x_F + \beta K')$$

$$dx_{F_2G}/dt' = 2\beta K'x_{GFG} + x_F x_{FG} + 2\alpha x_G x_{F_2} - x_{F_2G}(\alpha x_G + x_F + \beta K')$$

$$dx_{F_3G}/dt' = 2\beta K'x_{GF_2G} + x_F x_{F_2G} + 2\alpha x_G x_{F_3} - x_{F_3G}(\alpha x_G + x_F + \beta K')$$

$$dx_{F_4G}/dt' = 2\beta K'x_{GF_3G} + x_F x_{F_3G} + 2\alpha x_G x_{F_4} - x_{F_4G}(\alpha x_G + x_F + \beta K')$$

$$dx_{GFG}/dt' = \alpha x_G x_{FG} - 2\beta K'x_{GFG}$$

$$dx_{GF_2G}/dt' = \alpha x_G x_{F_2G} - 2\beta K'x_{GF_2G}$$

$$dx_{GF_3G}/dt' = \alpha x_G x_{F_3G} - 2\beta K'x_{GF_3G} \qquad (3)$$

Equations 3, together with the initial condition

$$x_A(t' = 0) = 1 \quad \text{for A = G}$$

$$x_A(t' = 0) = 0 \quad \text{for A} \neq \text{G}$$

may be solved numerically for any given values of K', α, and

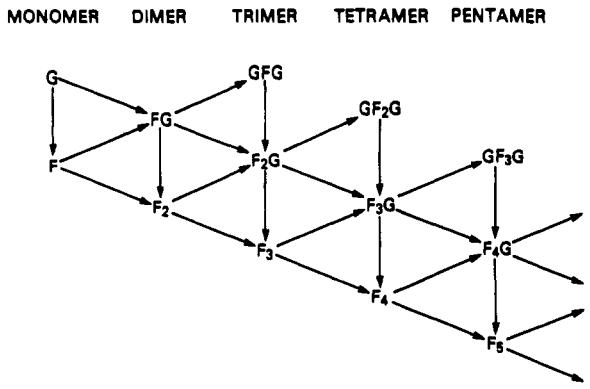

FIGURE 8: Network diagram for Scheme I. Arrows pointing downward represent a thrombin-catalyzed conversion of G to F. Arrows pointing upward and to the right represent the addition of a molecule of G to the "reactant" species (at the tail of the arrow). Arrows pointing downward and to the right represent the addition of a molecule of F to the reactant species. Reactions proceeding to the right represent an increase in the degree of oligomerization.

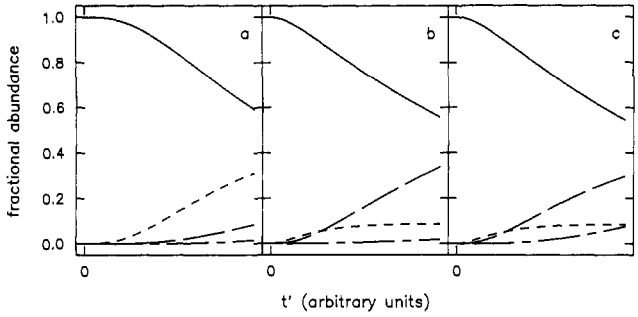

FIGURE 9: Fractional abundance of monomer (—), dimer (---), trimer (--), and tetramer+ (-·-·-) calculated as a function of t' as described in the text for three sets of parameter values. (a) $\alpha = 0$, β indeterminate; (b) $\alpha = 1$, $\beta = 0$; (c) $\alpha = 1$, $\beta = 1$.

β to yield the x_A as a function of time (t'). The values of the fractional abundances of monomer, dimer, trimer, and tetramer+ are then calculated by using

$$f_1 = x_G + x_F$$

$$f_2 = 2(x_{F_2} + x_{FG})$$

$$f_3 = 3(x_{F_3} + x_{F_2G} + x_{GFG})$$

$$f_{4+} = f_4 + f_5 = 4(x_{F_4} + x_{F_3G} + x_{GF_2G}) + 5(x_{F_5} + x_{F_4G} + x_{GF_3G}) \quad (4)$$

Simulations based on eq 3 and 4 were carried out for several combinations of parameter values representing different physical situations. To assure that we did not neglect significant amounts of oligomer higher than pentamer, all simulations were performed subject to the requirement that the maximum value of f_5 be much less than the maximum value of f_4 and constitute less than 1% of total oligomer.

In Figure 9a we have plotted the results of a simulation of oligomerization in the absence of the formation of fibrinogen–fibrin complexes ($\alpha = 0$). It may be seen that the fractional abundance of dimer increases more rapidly than that of trimer and achieves a much greater level during the time course of the simulation, in direct contrast to our experimental observations. This relationship between f_2 and f_3 was observed for all values of K' so long as $\alpha \ll 1$.

In Figure 9b, we plot the results of a simulation of oligomerization in which fibrinogen is permitted to form complexes with fibrin ($\alpha = 1$) and in which fibrinogen so complexed is "protected" from thrombin ($\beta = 0$). It may be seen that the calculated time dependence of dimer and trimer now resemble those observed experimentally much more closely than in Figure 7a, but the formation of tetramer and higher oligomers is significantly inhibited relative to that observed experimentally. Analysis of this simulation reveals that fibrin formed at early times is "trapped" by the large excess of fibrinogen and exists thereafter primarily in the trimeric complex GFG. Since these complexes are assumed not to dissociate, and since fibrinogen in the fibrinogen–fibrin complexes is assumed to be no longer accessible to thrombin, the amount of fibrinogen available for conversion to fibrin, and consequently the amount of fibrin available to undergo association to higher oligomers, is much less than would otherwise be the case.

In Figure 9c, we plot the results of a simulation of oligomerization in which fibrinogen is permitted to form complexes with fibrin ($\alpha = 1$) and in which complexed fibrinogen, like uncomplexed fibrinogen, is subject to the action of thrombin ($\beta = 1$). It may be seen that the results of this simulation are in satisfactory agreement with experimental observation. Analysis of the results reveals that the great bulk of each molecular weight species (ca. 90% or more) is made up of that complex containing the maximum number of fibrinogen molecules possible (one in the case of dimer and two in the case of trimer, tetramer, and pentamer).

Simulations have also been carried out for the intermediate case in which $\alpha = 1$ and $0 < \beta < 1$. As expected, the results are intermediate between those shown in parts b and c of Figure 9. Our data are therefore consistent, to within the uncertainty of measurement, with the assumption that the incorporation of a molecule of fibrinogen into an oligomer provides either no protection or partial protection against the proteolytic action of thrombin. However, it is doubtful that incorporation of a fibrinogen molecule into an oligomer provides complete protection against the action of thrombin.

Discussion

The formation of oligomers in fibrinogen solution following the addition of thrombin or other fibrinopeptide-releasing enzymes has been studied by a variety of techniques, prominent among them the measurement of light scattering in solution (Steiner & Laki, 1951; Mueller & Burchard, 1978; Hantgan & Hermans, 1979; Wiltzius et al., 1982) and the analysis of electron micrographs (Fowler et al., 1982; Janmey et al., 1983). It is notoriously difficult to interpret the results of light scattering in an unambiguous fashion when, as in the present case, the solution may contain a highly heterogeneous population of species and when the scattering of even a single species must in any event be interpreted within the context of an oversimplified representation of molecular shape. In contrast, electron microscopic studies offer the possibility of observing individual aggregates, but it is not clear that the relative abundances of different aggregates observed on the prepared grid in any way reflects the relative abundance of these species in the parent solution. Some species present in the parent solution may be absent from the grid, condensing during the process of drying the sample to form artifactual aggregates subsequently observed on the grid.

We feel that the chromatographic technique utilized here successfully avoids the uncertainties associated with the above methods. However, its use is predicated on the assumption that the distribution of oligomeric species calculated from the elution profile is a good approximation to the distribution of oligomeric species present in the parent solution at the time of thrombin inhibition. We base this assumption on the following experimental observations:

Smith (1980) reported that, under conditions similar to ours, SEC chromatograms of thrombin–fibrinogen solutions ob-

tained immediately following inhibition of thrombin were identical with chromatograms of the same solutions obtained 24 h after inhibition of thrombin. Preliminary experiments carried out in our laboratory showed that the elution profile was not significantly dependent upon the flow rate of solvent over the range 0.2–0.5 mL/min.

The two observations noted above, taken together, indicate that the distribution of oligomers calculated from the elution profile is stable at times comparable to or longer than elution times. But they do not eliminate the possibility that some oligomers present in the parent solution are more labile than other oligomers and that these labile oligomers dissociate during the process of chromatography. If such were the case, then the distribution of oligomers calculated from the elution profile would reflect the relative abundances of stable oligomers only, rather than all of the oligomers formed in the parent solution.

If there are stronger and weaker interactions between different monomeric species leading to the formation of oligomers, certainly the weakest (and most readily dissociable) ought to be that between fibrinogen and fibrin. Sherman et al. (1975) have shown that when ^{125}I-labeled fibrinogen is incubated with ^{131}I-labeled fibrin under conditions similar to those employed in our experiments (pH 7.4, moderate ionic strength, room temperature), and subsequently chromatographed on a size-exclusion column, a substantial fraction of the fibrinogen coelutes with fibrin in the void volume, while none of the fibrinogen elutes in the void volume in the absence of fibrin. This finding indicates that, under these conditions, the lifetime of fibrinogen–fibrin complexes, even in the absence of monomeric fibrinogen, is longer than or comparable to elution times encountered in the chromatographic separations of Sherman et al. (1975). Elution times were not specified by these authors, but on the basis of column dimensions given by them, together with the manufacturer's recommendations for the use of Sepharose columns, we estimate their elution times to be at least 10 times greater than our own. The results of Sherman et al. (1975) therefore suggest that the weakest complex-forming interactions likely to be present in our reaction mixtures at the moment of thrombin inhibition are sufficiently stable to survive our chromatographic separation essentially intact. Thus, the distribution of different molecular weight species present at the time of thrombin inhibition may be quantitated in an unambiguous and reasonably accurate manner via the procedure described earlier.

Using the TSK 4000SW column, we have been able to resolve dimeric and trimeric oligomers in solution but cannot distinguish between tetramers and higher oligomers in solution, which elute together in the void volume. Obviously this experimental limit severely restricts the amount of information that one can extract from modeling of the results. Moreover, the limitation of pore size prevents us from extending the study to longer durations of thrombin action, since aggregates that are too large become trapped within the column. We are presently exploring other types of high-performance size-exclusion columns that may permit the resolution of larger oligomers and extension of this study to longer durations of thrombin action.

One of the assumptions made in the kinetic model presented in the previous section was that both A peptides were removed from a fibrinogen molecule by thrombin in a concerted fashion, such that des-A fibrin never constitutes a significant fraction of total macromolecular content. Let us assume for the sake of argument that this is not the case and that the two A peptides are cleaved independently. Then the primary product of the initial encounter between a molecule of thrombin and a molecule of fibrinogen would be des-A fibrin. It follows that the first oligomer formed following the addition of thrombin to fibrinogen, and essentially the only oligomeric species formed at early times, would be the dimeric product of an association between des-A fibrin and either fibrinogen (in our model) or another molecule of des-A fibrin [in the model of Smith (1980), to be discussed]. This conclusion contradicts the observation that trimer, and not dimer, is the dominant oligomer formed at early times (Figure 6). As shown in the previous section, the small amount of dimer observed is well accounted for as consisting primarily of the complex GF.

The physical basis for the hypothesized concerted release of both A peptides from a molecule of fibrinogen is not difficult to envisage. We have recently been performing computer simulations of the motion of a particle undergoning a three-dimensional random walk in the presence of a mildly attractive spherical surface. It appears that an attractive potential of only 2 or 3 kcal/mol can suffice to keep the diffusing particle adjacent to the spherical surface until it has "explored" much or all of the surface area. (Details of these calculations will be described elsewhere.) Weakly attractive potentials of this magnitude are characteristic of the weak hydrophobic, electrostatic, and hydrogen-bonding interactions that would be expected to exist at the interface between two amphiphilic macromolecules in close contact. Thus, a thrombin molecule that has already catalyzed the release of one A peptide may quite possibly diffuse along and explore much of the surface of the fibrinogen, encountering the second A peptide (and catalyzing its release) before dissociating from the fibrin molecule and freely diffusing in the solvent.

In order to account for the predominance of trimeric over dimeric oligomers at early times following the addition of thrombin to fibrinogen, it is not necessary to assume that both A peptides are cleaved in a concerted fashion. One may instead assume that a molecule of des-A fibrin is identical with respect to oligomer formation with a molecule of fibrinogen; i.e., only a molecule of des-A_2 fibrin can associate with other molecules of des-A_2 fibrin, des-A fibrin, or fibrinogen. However, the physical basis for such an assumption is not clear, and moreover, the reaction scheme required to accommodate all possible association reactions leading to the formation of oligomers through pentamer would be far more complex that that shown in Scheme I and Figure 8.

A second assumption made in the kinetic model presented in the previous section was that, at short times, associations between oligomers may be neglected relative to associations between monomer and another monomer or oligomer. The reasons for this assumption are two: (a) The molar rate constant for formation of n-mer via association of monomer and $(n-1)$-mer is larger than that for formation of n-mer via association of j-mer and $(n-j)$-mer for any $j > 1$, because the larger, more anisometric species have smaller coefficients of translational and rotational diffusion (Tanford, 1961) and because the formation of n-mer from j-mer and $(n-j)$-mer is associated with a larger loss of translational and rotational entropy (i.e., more negative entropy of activation) than the formation of n-mer from monomer and $(n-1)$-mer (Steinberg & Scheraga, 1963). (b) Over the time span investigated in this study, the mole fraction of monomer is always much larger than that of any oligomer. (For example, from the data shown in Figure 6a, we calculate that the mole fractions of monomer, dimer, trimer, and tetramer at $\Delta t = 180$ s are approximately equal to 0.8, 0.07, 0.12, and 0.01, respectively). The rate of formation of an oligomer from two smaller oligomers will thus

Table II: Best-Fit Values of Parameters Obtained by Nonlinear Least-Squares Fitting of Equations 2a and 2c to Size-Exclusion Chromatographic Data Presented in Figure 1 of Smith (1980)[a]

	peaks 1 and 2			peak 3			peak 4			peak 5		
Δt (min)	v_1, v_2 (mL)	h_1, h_2	w_1, w_2 (mL)	v_3 (mL)	h_3	w_3 (mL)	v_4 (mL)	h_4	w_4 (mL)	v_5 (mL)	h_5	w_5 (mL)
0	20.3, 15.5	19.8, 27.7	9.0, 6.2									
60	21.1, 16.1	7.45, 20.6	5.3, 6.6	13.4	10.3	3.4	10.6	16.4	3.0	9.2	24.3	1.7
90	20.4, 15.9	8.7, 11.2	6.6, 7.4	13.8	13.0	4.2	10.4	57.0	2.5	9.0	20.2	1.1
120	(20.6), (16.1)	5.5, 8.0	6.9, 6.6	(14.0)	8.3	3.7	(11.0)	42.8	2.5	(9.1)	48.0	1.8
150	(20.7), (15.4)	6.7, 9.7	8.5, 5.7	(13.6)	5.8	1.2	11.0	73.0	3.7	(8.7)	19.1	1.7

[a] Values of the h_i are in arbitrary relative units. Parameter values enclosed in parentheses were not well determined by the data, so the values shown are the mean obtained from several preliminary fits. These parameters were then fixed at the indicated values, and the remaining parameters were allowed to vary to achieve a semiconstrained best fit.

be proportional to the product of two small numbers, while the rate of formation of the same oligomer from monomer and the next smaller oligomer will be proportional to the product of a relatively large number and a small number.

The earliest measurement of the amount and composition of soluble oligomers formed following addition of thrombin to fibrinogen (of which we are aware) was reported by Shainoff and Page (1962), who used rabbit fibrinogen and bovine thrombin. Following addition of a thrombin inhibitor prior to the appearance of fibrin gel, soluble oligomers were separated from monomer by selective precipitation in the cold. The supernatant was found to contain essentially pure fibrinogen. The pellet redissolved in fresh buffer upon reheating and was subsequently found to contain approximately 50% fibrin and 50% fibrinogen. They interpreted their findings as indicating that soluble oligomer was primarily a noncovalent dimeric complex of fibrin and fibrinogen. Their data are also compatible with the model presented here, if it is postulated that the precipitate of Shainoff and Page consisted of a mixture of trimers and higher oligomers in proportions such that the relative amounts of F and G were roughly equal.

Shainoff et al. (1970) performed sedimentation velocity experiments upon solutions of undegraded and partially degraded human fibrinogens that had been briefly exposed to the action of bovine thrombin prior to the addition of a thrombin inhibitor. They reported that the sedimentation pattern obtained using undegraded fibrinogen as substrate revealed the presence of two predominant species, the most abundant having a sedimentation coefficient equal to that of fibrinogen (8 S) and the less abundant having a sedimentation coefficient of 24 S. One cannot reliably estimate the frictional coefficients of oligomers whose fine structure is unknown, but it is probable that the frictional coefficient increases monotonically with increasing extent of linear association (Tanford, 1962). The 24S species is thus probably a trimer or larger oligomer rather than dimer. The results of the sedimentation experiments of Shainoff et al. (1970) therefore suggest that dimers are not the predominant oligomeric species formed at early times following the addition of thrombin to fibrinogen, in qualitative agreement with the results reported here.

The results of the present study and conclusions drawn from them may be most closely compared to those of an earlier chromatographic study of early stage oligomer formation in fibrinogen/fibrin solutions following addition of thrombin (Smith, 1980). Like ourselves, Smith obtained size-exclusion chromatograms of these solutions after various periods of thrombin action terminated by addition of a thrombin inhibitor (in his case, a synthetic oligopeptide derivative). However, his chromatograms were of substantially lower resolution than our own, being obtained with a 28-cm column of Bio-Gel A-5m, which the manufacturer's data state as having a maximum resolution of <5000 theoretical plates per meter, and the reaction conditions employed by him were somewhat different from those used by us. Smith's resolution of his chromatograms into contributions from different molecular weight species was qualitative rather than quantitative, and the mechanistic reaction scheme which he proposed to explain these chromatograms conflicts with that presented here. Smith attributes the stability of linear oligomers (i.e., lack of reactivity with fibrinogen) to the presence of a molecule of des-A fibrin at each end of the oligomer, while we attribute oligomeric stability to the "capping" of oligomer at each end with a molecule of fibrinogen. We have therefore quantitatively analyzed his data and model in an attempt to reconcile the two sets of observations.

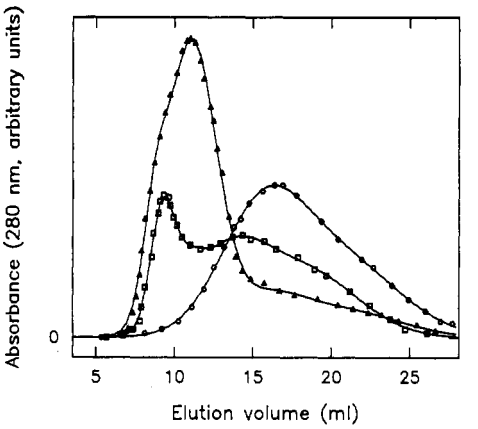

FIGURE 10: Size-exclusion chromatograms of fibrinogen solutions on which thrombin has been permitted to act for 0 (circles), 60 (squares), and 150 min (triangles). Data (symbols) are taken from Smith (1980). Continuous curves are calculated by using eq 2a and 2c with the parameter values given in Table II.

Enlargements of the chromatograms presented in Figure 1 of Smith (1980) were digitized and equations of the form of eq 2a–c with all symmetric Gaussian components were fit to the data set obtained from each chromatogram. (The data for Δt = 30 min and Δt = 220 min were not fit because of artifacts manifest in the appearance of these particular chromatograms.) It was found that two Gaussian functions of comparable area were required to quantitatively fit the data obtained for Δt = 0, where presumably only a single monomeric species is present. In order to fit the data sets obtained for $\Delta t > 0$, three additional Gaussian functions were employed, with elution volumes corresponding roughly to those designated by Smith as representing fractions f_2, f_x, and f_v (his notation). The parameter values determined by nonlinear least-squares fitting are presented in Table II, and chromatograms calculated by using eq 2a–c with these parameter values are shown together with the data for Δt = 0, 60, and 150 min in Figure

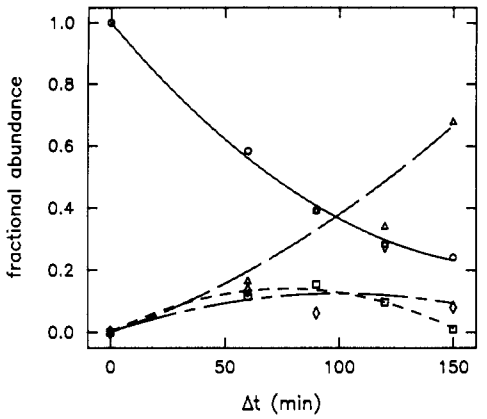

FIGURE 11: Fractional abundance of monomer (○) (—), dimer (□) (---), trimer (△) (−−), and tetramer+ (◇) (−·−) as a function of Δt calculated from the chromatographic data of Smith (1980) as described in the text. Points are the results of the calculations, and curves are quadratic smoothing functions fit to each set of points.

10. Fits to the data for $\Delta t = 90$ and 120 min are equally good.

In our interpretation of the decomposition described above, peaks 1 and 2 are jointly attributed to monomer, peak 3 is attributed to dimer, peak 4 is attributed to trimer, and peak 5 is attributed to tetrameric and larger species. The fractional abundance of each molecular weight species, calculated as described in the section on data analysis, using the parameter values presented in Table II, is plotted as a function of Δt in Figure 11. The uncertainty in parameter values determined by nonlinear least-squares fitting was much greater in the analysis of Smith's data than in the analysis of our own data, primarily because of the much lower resolution of his chromatographic technique, but also because of the additional uncertainty introduced into our analysis via the digitization of an artists' rendering of his data. Nevertheless, by varying peak positions, heights, and widths consistent with a reasonably good fit of eq 2a–c to the data, we found that any combination of parameter values capable of accommodating the observed chromatograms resulted in a time development of the various molecular weight species in qualitative agreement with that shown in Figure 11. In particular, the data seem to mandate that peak 4 (trimer) rapidly becomes the predominant soluble intermediate, while peak 3 (dimer) remains small, at no point exceeding about 15% of total soluble material. Given the much larger uncertainty inherent in Smith's results, and allowing for the longer time scale due to the substantially smaller concentration of thrombin used by Smith, the abundance curves shown in Figure 11 are surprisingly similar to those shown in Figure 6a,b. We thus claim that Scheme I can at least qualitatively account for the data presented in Figure 1 of Smith (1980).

The mechanism proposed by Smith (1980) to account for his data postulates that dimers arise from the association of two molecules of des-A fibrin. Further growth of the oligomer occurs only when thrombin releases the second A peptide from either of the des-A fibrin molecules comprising dimer, permitting trimer formation via the subsequent association of another des-A fibrin molecule. We have formulated a reaction scheme, analogous to that shown in Scheme I, based upon the postulates of Smith's model and have numerically solved the differential equations resulting from this reaction scheme to simulate the time evolution of oligomers as predicted by the model.[1] The results confirm the expectation on qualitative grounds (see above) that any model which both permits individual A peptides to be cleaved independently and permits des-A fibrin to associate with a single monomer or oligomer as a "half-activated fibrin" necessarily predicts that the dominant oligomeric species formed at early times following the addition of thrombin must be dimer. This prediction disagrees qualitatively with the results of our analysis of both our own data and the data of Smith (1980), as well as with the sedimentation results of Shainoff et al. (1970).

The well-known dependence of the rate and extent of gel formation and the structure of the resulting gel upon environmental variables such as temperature, pH, ionic strength, and the concentration of a variety of small molecules (Ferry & Morrison, 1947; Steiner & Laki, 1951) reflects the sensitivity of the underlying interactions between the aggregating macromolecules to alterations in the environmental variables.

These intermolecular interactions fall into at least three distinct classes: (a) interactions between the reactive site exposed upon release of the A peptides and the complementary site(s) on adjacent molecules; (b) interactions between the reactive site exposed upon release of the B peptides and the complementary site(s) on adjacent molecules; (c) interactions between adjacent regions of neighboring molecules in the aggregate that are not modified by the action of thrombin but that nonetheless contribute significantly to the free energy of aggregate formation. The three classes of interactions defined in this manner are both structurally and energetically distinct, and in the absence of detailed structural information about the regions of intermolecular contact associated with each class of interactions, there is no reason to presuppose that they respond in an identical, or even qualitatively similar, fashion to changes in any given environmental variable. (For example, an intermolecular interaction that is dominated by hydrophobic forces might be expected to become stronger with increasing temperature, while one dominated by electrostatic forces would be expected to weaken with increasing temperature.)

It is much more probable that changes in environmental variables lead not only to an alteration in the overall free energy of aggregation but also to an alteration in the relative contributions of each of the three types of interactions to the total free energy of aggregation. If this is the case, then the structure of the predominant intermediates formed during the process of fibrin gelation is at least as subject to variation as is the structure of the final gel itself. It follows that references to "the" mechanism of fibrin gel formation are misleading, as they imply that it is independent of the conditions under which the reaction is carried out. Even under the conditions of the present study, two distinctly different limiting mechanisms of oligomer formation may be deduced from the model reaction scheme (Scheme I), depending upon the initial concentrations of thrombin and fibrinogen. When the concentration of thrombin is so small that the rate of conversion of G to F is much smaller than the rate with which G may associate with a growing oligomer, then the predominant pathway for growth of an oligomer at early times would be

$$G \xrightarrow{(T)} F \xrightarrow{+G} FG \xrightarrow{+G} GFG \xrightarrow{(T)} F_2G \xrightarrow{+G} GF_2G \xrightarrow{(T)} \cdots$$

On the other hand, when the concentration of thrombin is so great that the rate of conversion of G to F is much larger than the rate with which G may associated with a growing oligomer, then the predominant pathway for growth of an oligomer at early times would be

$$G \xrightarrow{(T)} F \xrightarrow{+F} F_2 \xrightarrow{+F} F_3 \xrightarrow{+F} F_4 \xrightarrow{+F} \cdots$$

[1] Details of this reaction scheme and results of the simulation may be obtained from A.P.M. upon request.

In summary, we have presented high-resolution size-exclusion chromatographic data and an analysis of these data that provides a quantitative measure of the fractional abundance of monomeric and oligomeric species formed during early stages of thrombin action on bovine fibrinogen. We have also presented a kinetic model for oligomer formation based upon the notion that reactive monomers and oligomers may associate with fibrinogen molecules (up to a maximum of two fibrinogens per oligomer) as well as with other reactive species and that such mixed oligomers comprise the bulk of oligomeric species present in early stages of thrombin-initiated fibrin gel formation. This model accounts semiquantitatively for the data presented here and accounts qualitatively for the chromatographic data previously reported by Smith (1980).

We have recently begun exploring the relationship between the kinetics of oligomer formation at short times following the addition of thrombin and the characteristic lag time preceding the appearance of firm fibrin gel (t_{gel}). If one assumes that t_{gel} is proportional to the time required to deplete the total mass of monomers and oligomers of degree of polymerization ≤ 5 by a certain critical amount (which is, by definition, equal to the amount of time required to form the same critical amount of oligomers with degree of polymerization >5), then the model presented here can qualitatively account for the biphasic dependence of t_{gel} upon initial fibrinogen concentration at low thrombin concentration remarked upon in the introduction. We are presently attempting to formulate a model that can provide a comprehensive quantitative correlation between the kinetics of oligomer and gel formation.

ACKNOWLEDGMENTS

We thank Drs. M. S. Lewis, P. D. Ross, and especially H. A. Saroff for critically reviewing the initial draft of this paper.

Registry No. Thrombin, 9002-04-4.

REFERENCES

Ackers, G. K. (1970) *Adv. Protein Chem. 24*, 343–446.

Blömback, B., Hessel, B., Hogg, D., & Therkildsen, L. (1978) *Nature (London) 275*, 501–505.

Brass, E. P., Forman, W. B., Edwards, R. V., & Lindan, O. (1976) *Thromb. Haemostasis 36*, 36–48.

Ferry, J. D., & Morrison, P. R. (1947) *J. Am. Chem. Soc. 69*, 388–400.

Fowler, W. E., & Erickson, H. P. (1979) *J. Mol. Biol. 134*, 241–249.

Fowler, W. E., Hantgan, R. R., Hermans, J., & Erickson, H. P. (1981) *Proc. Natl. Acad. Sci. U.S.A. 78*, 4872–4876.

Hall, C., & Slayter, H. (1959) *J. Biochem. Biophys. Cytol. 5*, 11–15.

Hantgan, R. R., & Hermans, J. (1979) *J. Biol. Chem. 254*, 11272–11281.

Janmey, P. A., Erdile, L., Bale, M. D., & Ferry, J. D. (1983) *Biochemistry 22*, 4336–4340.

Krell, W., Mahn, I., & Muller-Berghaus, T. G. (1979) *Thromb. Res. 14*, 299–310.

Magar, M. E. (1972) *Data Analysis in Biochemistry and Biophysics*, Academic Press, New York.

Martinelli, R. A., & Scheraga, H. A. (1980) *Biochemistry 19*, 2343–2350.

Mueller, M., & Burchard, W. (1978) *Biochim. Biophys. Acta 537*, 208–225.

Sasaki, T., Page, I. H., & Shainoff, J. R. (1966) *Science (Washington, D.C.) 152*, 1069–1071.

Scheraga, H. A. (1983) *Ann. N.Y. Acad. Sci. 408*, 330–343.

Shainoff, J. R., & Page, I. H. (1962) *J. Exp. Med. 116*, 687–707.

Shainoff, J. R., Lahiri, B., & Bumpus, F. M. (1970) *Thromb. Diath. Haemorrh., Suppl. 39*, 203–217.

Sherman, L. A., Harwig, S., & Lee, J. (1975) *J. Lab. Clin. Med. 86*, 100–111.

Shinowara, G. Y. (1966) *Biochim. Biophys. Acta 113*, 359–374.

Smith, G. F. (1980) *Biochem. J. 185*, 1–11.

Steinberg, I. Z., & Scheraga, H. A. (1963) *J. Biol. Chem. 238*, 172–181.

Steiner, R. F., & Laki, K. (1951) *Arch. Biochem. Biophys. 34*, 24–37.

Tanford, C. (1961) *Physical Chemistry of Macromolecules*, Wiley, New York.

Wiltzius, P., Kanzig, W., Hofmann, V., & Straub, P. W. (1981) *Biopolymers 20*, 2035–2049.

Yudelman, I., Spanondis, K., & Nossel, H. L. (1974) *Thromb. Res. 5*, 495–509.